LUND UNIVERSITY

FACULTY OF SCIENCE

Saturated planar laser-induced fluorescence using sinusoidal intensity modulation

Klara Lozani Gerdhem

Thesis submitted for the degree Bachelor of Science
Project duration: 2 months
Supervised by: Dr. Elias Kristensson and Vassily Kornienko

Department of Physics, Division of Combustion Physics, June 2023

Saturated planar laser-induced fluorescence using sinusoidal intensity modulation

by Klara Lozani Gerdhem

LUND
UNIVERSITY

Thesis submitted for the degree Bachelor of Science, General Physics
Project duration: Four months at half-speed
Thesis advisors: Dr. Elias Kristensson and Vassily Kornienko
Division of Combustion Physics

Abstract

Saturated laser-induced fluorescence (saturated LIF) has been the topic of some research, however mainly regarding laser diagnostic methods conducted on flames. A few papers have discussed saturated LIF with the purpose of producing saturation curves of different fluorescent elements. The utilised methods in these cases have involved manually increasing the laser intensity and detecting the fluorescence intensity after each increment. The method proposed here involves conducting saturated planar laser-induced fluorescence, or saturated PLIF, using structured light in order to increase the efficiency of producing a saturation curve. Due to the intensity distribution of the structured light, it is possible to obtain a range of intensities from a single measurement. The response of the detected fluorescence signal is then compared to the signal of the laser which irradiates the sample in order to produce a saturation curve. To the best of the author's knowledge, no previous studies have used the method described above. Using this method, saturation curves for Rhodamine B, Rhodamine 560, Fluorescein, and Coumarin 153 were obtained using only one image of the saturated sample and one reference image in each case. The saturation curves were all distinguishable from each other, thus strongly suggesting that the method in this project can be used to differentiate between fluorophores. Clear dependencies on lifetime and absorption cross section were detected when analysing the saturation curves. This observation indicates that the method used in the project has the potential of being used in several cases where laser diagnostic methods for analysing fluorophores are wanted.

Acknowledgements

The time I have spent at the Department of Combustion Physics has been the best time of my bachelor's program. Therefore I want to thank everybody in the department for making me feel welcome and for creating such a nice and friendly work environment. I particularly want to thank my supervisors Elias Kristensson and Vassily Kornienko. Elias, thank you for giving me the opportunity to work on the most interesting project I have ever worked on. Your helpful and pedagogical attitude opened up interesting discussions and made me feel welcome to ask questions whenever I needed. You always motivated me to do my very best and to find new creative ways of thinking. Vasse, thank you for always helping me and for always being there to answer all of my questions, big and small. Your positive attitude and interest in the subject made the project even more enjoyable. It also made me more motivated in my work than ever. I also want to thank Julia Lövgren, Love Kildetoft, Alexander Petersson and Isa Hendriks for creating such a great community in the office. Finally, I want to thank my family and friends for always being there and supporting me, both in good times and more stressful times. I especially want to thank you Max for your support and our long and interesting discussions about the project, which helped me a great deal.

Abbreviations

CW	**C**ontinous **W**ave
DOE	**D**iffractive **O**ptical **E**lement
FFT	**F**ast **F**ourier **T**ransform
LIF	**L**aser **I**nduced **F**luorescence
PLIF	**P**lanar **L**aser **I**nduced **F**luorescence

Table of Contents

1 Introduction

New methods of studying both objects and phenomena are always sought after in the field of physics. Laser-induced fluorescence (LIF) is a well-known laser diagnostic method, frequently used in research. The physical process of fluorescence can be described with a diagram, such as the one shown in Figure 1(b). LIF can also be conducted using a laser sheet. The method is then known as planar laser-induced fluorescence, or PLIF. Figure 1(a) shows a sample of fluorophores used to conduct PLIF. It is possible to conduct LIF or PLIF in such a way that the irradiated sample becomes saturated. These diagnostic methods are known as saturated LIF and saturated PLIF and are not as thoroughly investigated as LIF or PLIF, thus containing possible unknown potential.

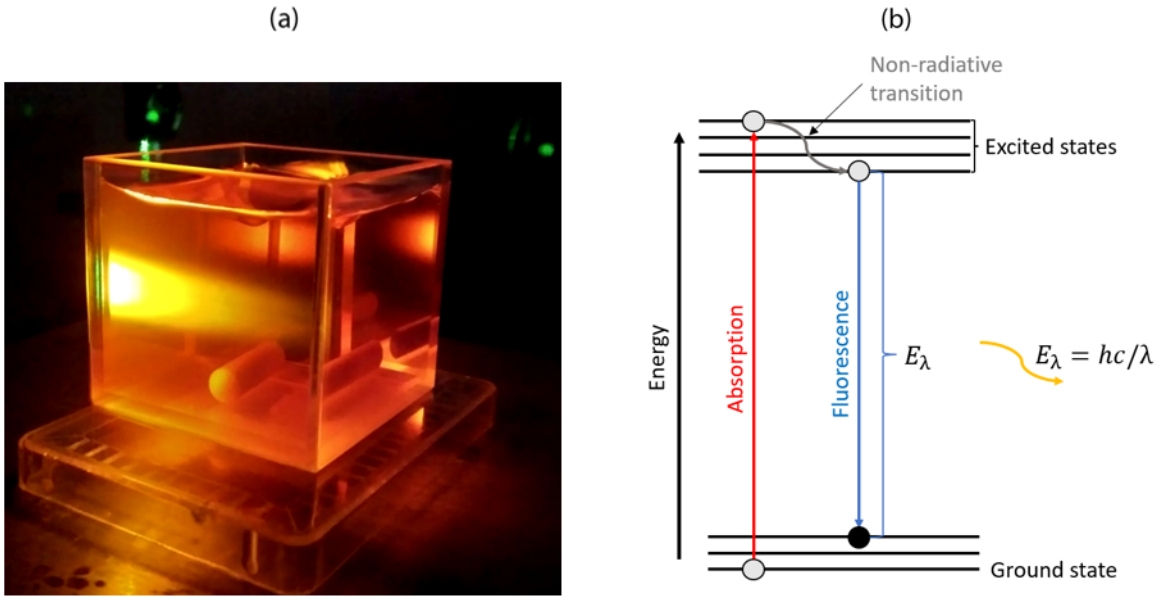

Figure 1: Two figures illustrating fluorescence. (a) shows a picture of an illuminated fluorophore in a setup where PLIF is preformed. (b) shows a diagram graphically describing fluorescence. E_λ denotes the energy difference between the two marked energy states.

Saturated LIF or saturated PLIF is performed by irradiating a fluorescent sample with a high-intensity laser beam. Saturation is achieved when the sample becomes strongly excited. By detecting the fluorescence intensity and plotting it against the intensity of the incoming laser it is possible to obtain a so-called saturation curve. An example of a saturation curve is shown in Figure 2. There the saturation curve (consisting of red crosses) is compared to the linear curve obtained when LIF or PLIF is used. The main difference between the two curves is that the saturation curve behaves non-linearly and converges to a constant value at high laser intensities.

Saturated LIF has previously been used mostly in flame measurements as a way to avoid data being affected by collisional quenching, which is deexcitation due to collisions with other molecules. There has also been some research done on liquid fluorescent substances where saturation curves have been measured [1]. However, no research using saturated LIF (or saturated PLIF) with the main purpose of obtaining saturation curves

for analysis has been conducted. Unfortunately, the existing way of producing saturation curves involves increasing the laser intensity manually in certain increments. Several measurements are thus required to produce just one curve, resulting in the process being inefficient. A way to improve efficiency is by utilizing structured light with sinusoidal intensity modulation.

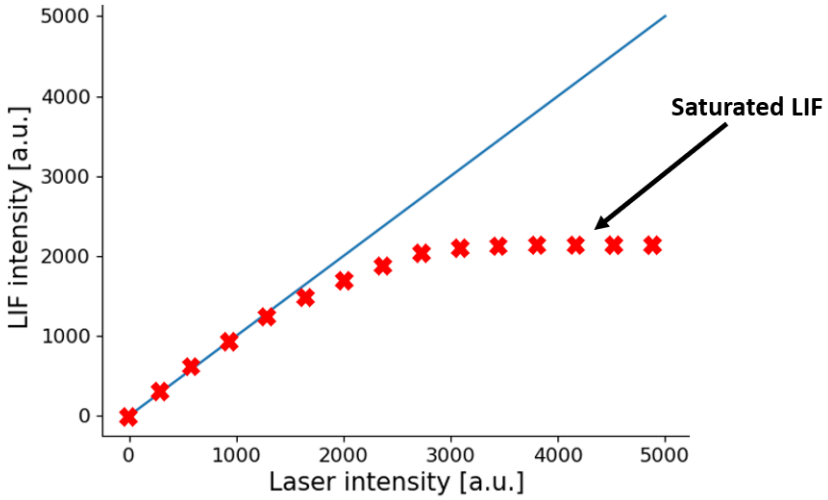

Figure 2: Curves showing the difference between LIF (or PLIF), yielding the blue linear curve, and saturated LIF (or saturated PLIF), yielding the red crosses.

Structured light is created through a grating being imaged on the laser beam, resulting in a range of different spatially separated intensities irradiating the sample during each measurement. A sinusoidal structure can be achieved by manually removing higher orders at the location of the Fourier domain. This project will investigate how structured light can be used in combination with saturated PLIF, in order to create a more efficient method for producing saturation curves.

A setup including a nanosecond laser and a DOE, creating structured light, will be used in order to conduct saturated PLIF with sinusoidal intensity modulation. Several fluorophores will be studied with the purpose of extracting their individual saturation curves. These curves will then be analysed in order to investigate how different physical properties of the fluorophores affect their saturation curves. These properties, such as lifetime, concentration, and absorption spectra, will be revealed with snapshot speed.

The theory used to conduct the proposed method is presented in Section 2. The subjects included in this section are LIF, PLIF, saturated LIF, saturated PLIF and the concept of structured light. Section 3 discusses both the experimental method and the methods used to simulate results and analyse data. The results are presented in Section 4, along with discussions of said results. Finally, Section 5 includes a conclusion, while Section 6 includes an outlook discussing the future possibilities of the proposed method.

2 Theory

2.1 Laser-induced fluorescence (LIF)

Fluorescence is a process where an atom or molecule is excited by an external light source and after some time emits light due to a spin neutral deexcitation [2]. An atom or molecule reacting in that way is known as a fluorophore. Depending on the wavelength of the emitted light, the process is known as either fluorescence or resonant fluorescence. The prior denotes the process where the emitted light has a shift in wavelength relative to the incoming light. In the latter case, the wavelength is unaltered. The excitation can be achieved through various methods, where one is photon absorption.

The most convenient way to achieve excitation by photon absorption is to use lasers since they have high intensities and can be focused easily [2]. When lasers are used in this manner the process is known as laser-induced fluorescence (LIF). This process begins with the absorption of a photon, which excites the fluorophore. After a certain period of time, known as the fluorescence lifetime, the fluorophore deexcites and emits a photon. Resonant fluorescence is observed more seldom which implies that the occurrence of non-radiative shifts in the excited states is common. For a two-level system, the excitation can be described with the following expression

$$N_1 + h\nu \xrightarrow{B_{12}I_\nu} N_2 \tag{1}$$

where N_1 is the population of the lower state, N_2 is the population of the higher state, B_{12} is the Einstein coefficient for excitation and I_ν is the intensity of the exciting light [2, 3]. The radiative deexcitation of the fluorescence transition can be described in a similar way

$$N_2 \xrightarrow{A_{21}} N_1 + h\nu \tag{2}$$

where A_{21} is the Einstein coefficient for spontaneous emission. However, deexcitation can occur due to other processes as well [2]. One of these processes is stimulated emission. It behaves according to Equation (2) with the exception that A_{21} is replaced with B_{21} which is the Einstein coefficient for stimulated emission.

LIF has several advantages in the field of laser diagnostics, including a strong signal which yields a high detection sensitivity. Despite this, the technique has several difficulties. One of the most predominant ones is collisional quenching of the excited states [4]. This non-radiative reaction occurs due to particle collision and causes deexcitation of the excited fluorophore. Therefore it competes with fluorescence and is a pronounced source of error when conducting LIF [5]. The process can be explained in the following way

$$N_2 + M \xrightarrow{Q_{21}} N_1 + M^* \tag{3}$$

where M is the collision partner, Q_{21} is the total quenching probability, and * suggest that the collision partner might be excited after the collision [2, 3]. A proposed solution to the problem with quenching is the usage of saturated LIF instead [4].

2.1.1 Planar laser-induced fluorescence (PLIF)

If LIF is conducted using a laser sheet, the experimental process is known as planar laser-induced fluorescence, or PLIF [2]. PLIF is used to conduct 2-D fluorescence imaging of samples. The method is often used to measure concentrations of radicals in flames, although it has many different areas of usage. Just as with LIF, PLIF is affected by collisional quenching, a problem which can be solved by using saturated PLIF.

2.2 Saturated laser-induced fluorescence (Saturated LIF)

Saturation of a fluorophore can be achieved by increasing the laser irradiance I_ν until it becomes much larger than the saturation irradiance I_ν^{sat} [2]. When saturation has been reached, a change in irradiance will not change the fluorescence intensity. This behaviour is known as saturated laser-induced fluorescence, or saturated LIF.

Saturated LIF can be described using Equations (1), (2) and (3). By combining these equations, it is possible to obtain the following rate equations

$$\frac{dN_1}{dt} = -N_1 b_{12} + N_2(b_{21} + A_{21} + Q_{21}) \tag{4}$$

$$\frac{dN_2}{dt} = N_1 b_{12} - N_2(b_{21} + A_{21} + Q_{21}) \tag{5}$$

where b_{12} and b_{21} are described according to the expression

$$b = \frac{BI_\nu}{c} \ .$$

These rate equations describe how the populations of the two levels N_1 and N_2 change over time. Assuming that the net population loss is negligible, it holds that $N_1 + N_2 = N_1^0$, where N_1^0 is the total number of particles [2]. If it is also assumed that the population of N_2 is negligible prior to excitation and that the case observed is one where a steady state has been achieved, which corresponds to $\frac{dN_1}{dt} = \frac{dN_2}{dt} = 0$, then the following can be stated

$$N_2 = N_1^0 \frac{b_{12}}{b_{12} + b_{21}} \frac{1}{1 + \frac{A_{21}+Q_{21}}{b_{12}+b_{21}}} \ . \tag{6}$$

This can be rewritten as

$$N_2 = N_1^0 \frac{B_{12}}{B_{12} + B_{21}} \frac{1}{1 + \frac{I_\nu^{sat}}{I_\nu}} \tag{7}$$

where

$$I_\nu^{sat} = \frac{(A_{21} + Q_{21})c}{B_{12} + B_{21}} \ . \tag{8}$$

Because the fluorescence signal power I_F is equal to $N_2 A_{21}$ it is possible to express Equation (7) as

$$I_F = N_2 A_{21} = A_{21} N_1^0 \frac{B_{12}}{B_{12} + B_{21}} \frac{1}{1 + \frac{I_\nu^{sat}}{I_\nu}} \ . \tag{9}$$

This can be simplified by setting $k = A_{21} N_1^0 \frac{B_{12}}{B_{12}+B_{21}}$, which yields

$$I_F = k \frac{1}{1 + \frac{I_\nu^{sat}}{I_\nu}} \ . \tag{10}$$

Thus, if $I_\nu \gg I_\nu^{sat}$ Equation (10) will become $I_F = k$. The result suggests that the fluorescence signal power will approach a constant value when the intensity of the exciting light I_ν becomes large enough in comparison to the saturation irradiance I_ν^{sat}.

Saturated LIF has mainly been used to avoid an unknown background due to collisional quenching when conducting LIF on flames [4]. This is because the rates of absorption and stimulated emission become so large that the rate of the collisional quenching is negligible in comparison [2]. The fluorescence signal yield is also maximized when conducting saturated LIF. However, there are some difficulties with the method, the most prominent one being that saturation is challenging to achieve. This can either be because a very high intensity is needed, or because of how the absorption cross section of the fluorophore relates to the wavelength of the exiting light.

Previous research on saturated LIF has shown that the emission rate E from a fluorescent sample follows this expression

$$E \propto \left[\frac{I\sigma}{(I\sigma + k_f)} \right] [1 - \exp\{-(I\sigma + k_f)t_p\}] \tag{11}$$

where I is the illumination photon flux, σ is the absorption cross section, k_f is the fluorescent decay rate, and t_p is the laser pulse length [6]. It is also worth noting that $k_f = 1/\tau$, where τ is the fluorescence lifetime. Thus for long pulse lengths, or continuous light, $t_p \gg \tau$, which results in

$$E \propto \left[\frac{I\sigma}{(I\sigma + k_f)} \right] \ . \tag{12}$$

Short pulse lengths however, where $t_p \ll \tau$, will give the following proportionality

$$E \propto [1 - \exp\{-(I\sigma + k_f)t_p\}] \ . \tag{13}$$

The exponential dependence is more effective at reaching saturation [6]. Therefore it is suggested that pulsed lasers are preferable when saturated LIF is wanted.

By plotting the fluorescence signal from a saturated sample against the intensity of the incoming laser, it is possible to obtain a saturation curve [7]. When working with saturated LIF, such a curve is acquired by changing the intensity of the laser by certain increments and measuring the fluorescence yield for each intensity. The obtained data points are then collected and used to plot the saturation curve. The main disadvantage of this process is that it is implied to be inefficient.

2.2.1 Saturated planar laser-induced fluorescence (Saturated PLIF)

Saturation using PLIF is known as saturated planar laser-induced fluorescence, or saturated PLIF [8]. Because 2-D measurements easily can be conducted using PLIF, saturated PLIF is an alternative method for producing such measurements, while avoiding sources of error such as collisional quenching. The underlying physics of saturated PLIF is the same as for saturated LIF. Therefore, Equation (10) and (11) are applicable on saturated PLIF. However, due to the similarities between saturated LIF and saturated PLIF, the issues regarding inefficiency of producing saturation curves is a problem for saturated PLIF as well.

2.3 Structured light

To avoid the measurement techniques mentioned in the section above when measuring saturated LIF and saturated PLIF, structured light can be used. The structured light will then be used to improve the efficiency of the measurements. How measurements involving structured light can be conducted will be described in this section.

Structured light is created by imaging a grating with a laser beam [9]. The grating then imprints a periodic line pattern on the beam. A type of grating that can be used is a diffractive optic element (DOE), which is an optical element that splits the laser beam [10]. A DOE consists of a specific multi-step surface, which pattern can differ greatly between different DOE:s. The intensity distribution of the DOE depends on the properties of the structure, and thus also varies between different DOE:s. For example, light with sinusoidal intensity modulation can be created using a DOE.

Another type of grating which can be used is a Ronchi grating [5]. This grating has alternating opaque and transmissive strips, yielding an image of a square wave when illuminated. Because of these properties, only 50% of the light reaching the Ronchi grating will be transmitted. It is however possible to alter the shape of the structured light created by a Ronchi grating. Square waves have Fourier transforms which includes many high frequencies, so blocking a number of these will give an altered shape.

The presence of optics, in the form of lenses, is convenient to use when conducting imaging of structured light, partly since the lenses can be used to modify the structure of the light [5]. The thin-lens approximation states that

$$\frac{1}{S_1} + \frac{1}{S_2} = \frac{1}{f}, \tag{14}$$

where S_1 and S_2 are the distance from the lens to the object and the image respectively, and f is the focal length of the lens [11]. A special case of the lens formula is used in a 4-f imaging system [12]. Such a system is shown in Figure 3. The first lens is placed one focal length away from the object. According to Equation (14), this placement implies $S_2 \approx \infty$, which corresponds to the image being found in infinity. The second lens is placed one focal length from where the image is wanted, thus resulting in $S_1 \approx \infty$. The object will then be imaged on the screen shown in the right corner of Figure 3 [12].

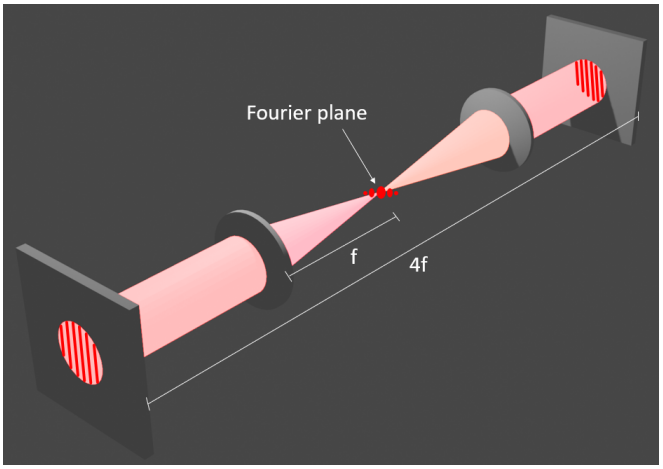

Figure 3: A model of a 4-f imaging system using a Ronchi grating. Both lenses in this system has the same focal length.

By using a lens, it is possible to obtain the diffraction pattern of the object that is to be imaged one focal length from the lens [12]. This diffraction pattern is the spatial Fourier transform of the object that is illuminated. When taking the Fourier transform of the light wave, the different Fourier components, over a frequency scale, will be found. The location where the Fourier components can be found is called the Fourier plane. In the 4-f imaging system, the Fourier plane will be found precisely in between the two lenses, which can be seen in Figure 3. By placing a filter in the Fourier plane, certain Fourier components can be blocked [12]. Thus, if the filter is designed and placed in a certain way, it is possible to block all Fourier components apart from the first positive and negative one. This type of blocking will then result in an image of a perfect sine wave. Thus, with this method it is possible to modify the square wave created by a Ronchi grating into a sine wave.

It is suggested that the use of structured light increases the efficiency when measuring saturated LIF [5]. One reason for this is that the Fourier transform of the fluorescence signal then can be analysed to determine whether saturation has been achieved or not. In the case that it has been achieved, additional Fourier components, other than the first-order components, will be observed. For example, if structured light was to be used, I_ν in Equation (10) would be a sine wave, while I_F would be a sine wave modified due to saturation. Another reason for the increased efficiency is that the intensity distribution of structured light varies over space, resulting in the sample being irradiated with light including different intensities in each measurement. Therefore, it is theoretically possible to create a saturation curve from just one measurement of a saturated sample; drastically increasing the efficiency of creating a saturation curve.

3 Method

3.1 Simulation code

All code in this project was written in Python [13]. The code described in this subsection can be found in Appendix B. The purpose of the simulation code for this project was for it to be a model of the expected experimental results. The experiment was expected to give

values of the incoming and outgoing intensities. Here the incoming intensity corresponds to the intensity of the laser and the outgoing intensity corresponds to the fluorescence intensity. Therefore, a way to obtain saturation curves from that information was desired. To achieve this, three different types of saturation curves were plotted; one linear, one square root-shaped, and one described by Equation (10). The saturation curves were created using a normalised sine wave, representing the laser signal, as variable in the expressions for the three shapes. The simulations of the fluorescence signals were created by plotting the y-axis of the saturation curve against the x-axis of the normalised sine wave. Finally, fast Fourier transforms, or FFTs, were made of the laser and fluorescence intensity signals using the fft package from the SciPy library [14].

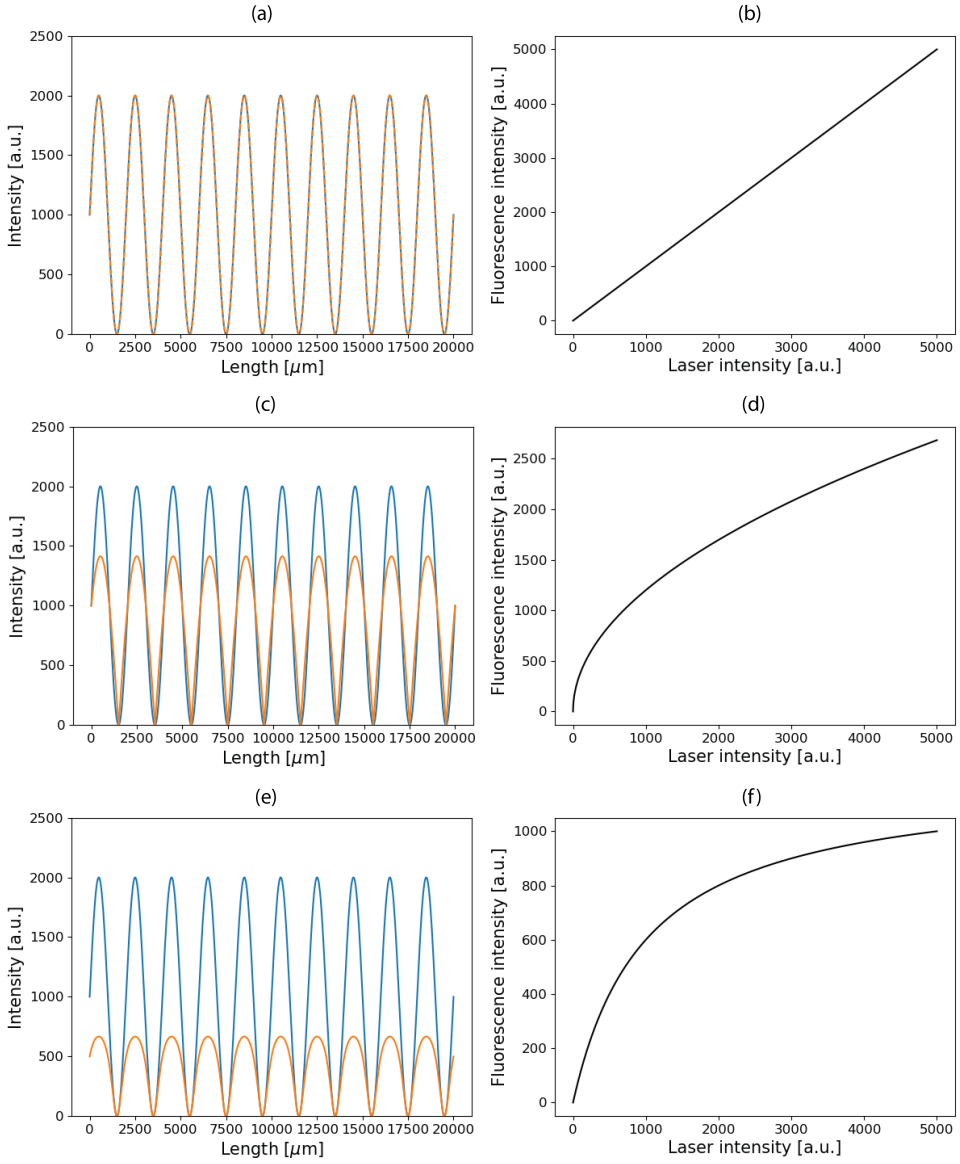

Figure 4: Simulations of different laser signals (blue sine curves), fluorescence signals (orange curves) and saturation curves. (a) shows the laser and fluorescence signals for a linear saturation curve (on the form $y = k \cdot x$), which is shown in (b). (c) shows the signals for a square-root saturation curve (on the form $y = k \cdot \sqrt{x}$), shown in (d). (e) shows the signals for a saturation curve described by Equation (10), shown in (f).

When comparing the fluorescence signals shown in Figures 4(a), 4(c) and 4(e), a clear difference can be observed between the signal in Figure 4(a) and the other two signals. This can be connected to the fact that the response curves in the two latter cases are non-linear, while the response curve in the first case is linear. The response curve in Figure 4(d) is more linear than the response curve shown in Figure 4(f). This linear behaviour is mostly observed at higher laser intensities. As a consequence, the fluorescence signal in Figure 4(c) is not as distorted compared to the laser signal. The main visible difference between the two signals is that the maximum fluorescence intensity is lower compared to the maximum laser intensity. The fluorescence signal corresponding to the response curve described by Equation (10), can be seen in Figure 4(e). In this case, a clear difference between the laser signal and the fluorescence signal can be observed, both regarding shape and maximum intensity. The different behaviours of the fluorescence signals, compared to the laser signal, in the cases of the two latter response curves can also be observed in Figures 5(b) and 5(c). These Fourier transforms show an increased number of peaks compared to the Fourier transform in Figure 5(a), suggesting that the fluorescence signals yielded by the response curves in Figures 4(d) and 4(f) are not perfectly sinusoidal.

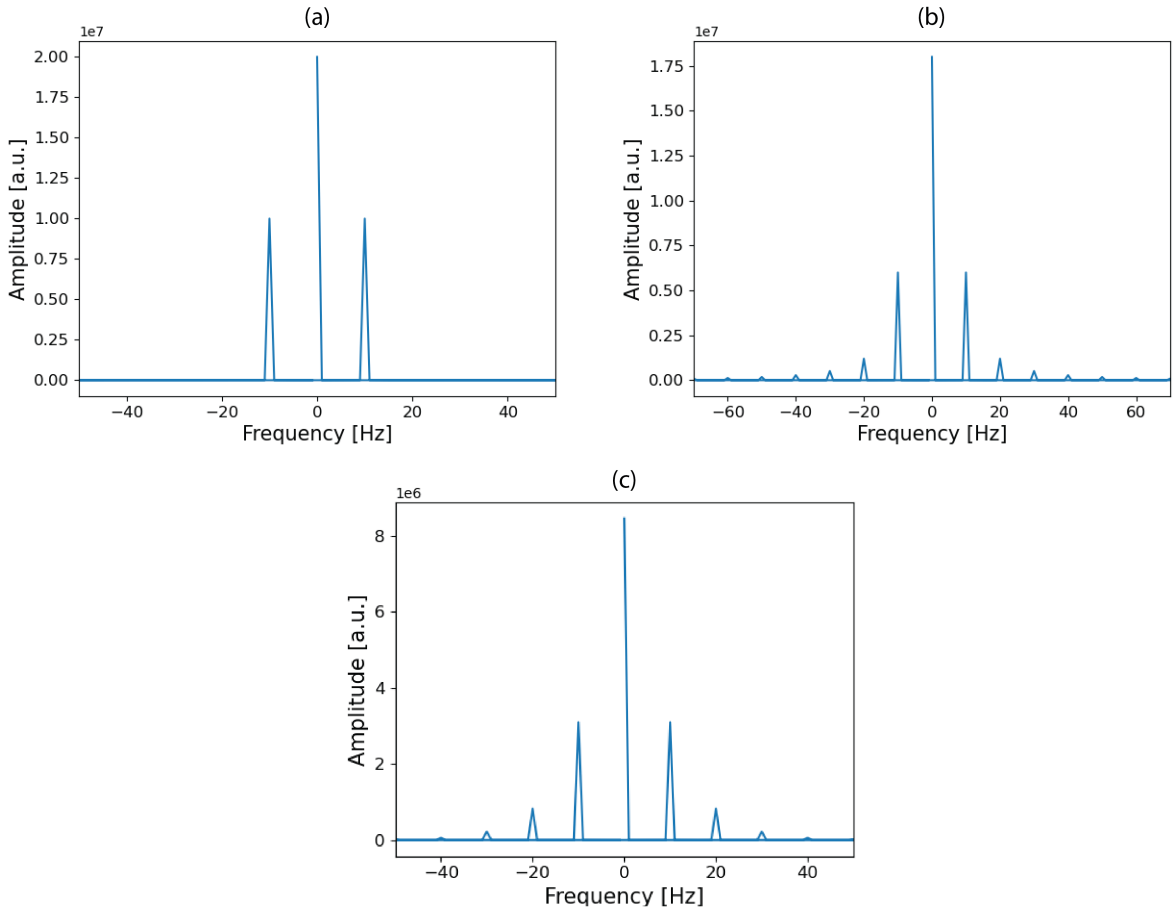

Figure 5: Fourier transforms of fluorescence signals given by three different saturation curves. (a) shows the Fourier transform for the case of a linear curve, (b) shows the Fourier transform for the case of a square-root curve and (c) shows the Fourier transform for the case of a curve described by Equation (10).

3.2 Experimental setup

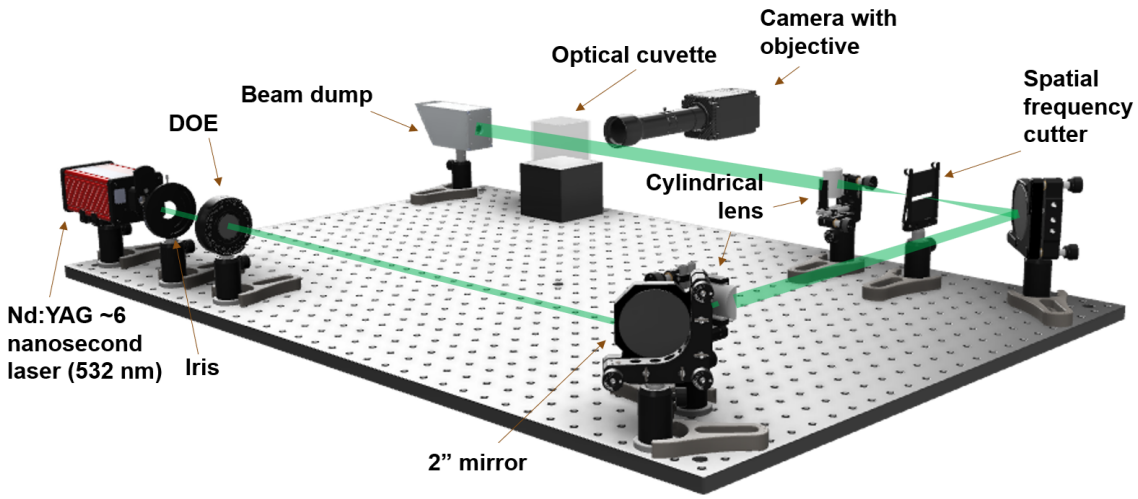

Figure 6: The experimental setup shown from the side.

A model of the setup described here is shown in Figure 6. To achieve saturation a Quantel Q-smart 850 pulsed Nd:YAG laser with a pulse length of ∼6 ns and a wavelength of 532 nm was used in the setup [15]. An iris was placed after the laser for aligning and adjusting the amount of light passing through the setup. Since the purpose of the experiment was to study the saturation of a fluorophore using structured light, a structured laser sheet was created using a DOE and two cylindrical lenses placed orthogonal to each other. The purpose of the first cylindrical lens, which had a focal length of 450 mm, was to create an image of the DOE, while the second lens, which had a focal length of 700 mm, was used to focus the created laser sheet. Two 2" mirrors angled 45° were situated in the setup to direct the laser sheet in the wanted directions. To ensure that the structured laser sheet had a sinusoidal modulation, a spatial frequency cutter was located one focal length after the first lens. The purpose of this component was thus to block higher orders produced by the DOE.

The sample, which was to be studied, was kept in a ∼5 cm^3 optical cuvette. It was then possible to conduct imaging of the sample by placing an Andor Luca S 658M camera with OEM Housing and an attached Edmund optics GoldTL™ Telecentric Lens objective with a PMAG of 0.5X next to the cuvette [16, 17]. The camera could be positioned in two ways, either facing the side of the cuvette or the top of it. In the first case, the cylindrical lenses were rotated so that a vertical laser sheet was created, and in the latter case, so that a horizontal sheet was created. A beam dump was located a certain distance after the cuvette to prevent light from the laser to be scattered around in the room and to dump the laser energy.

3.3 Attaining saturation

To be able to investigate possible differences between the saturation curves of different fluorophores, four fluorophores were selected for the measurements. Three of them, Rhodamine B, Rhodamine 560, and Fluorescein, all had absorption spectra which are non-zero at the wavelength of the laser. The fourth, Coumarin 153, have an absorption

spectrum which is zero at the wavelength of the laser. Coumarin 153 was thus selected to investigate how the saturation curve of a fluorophore would depend on the absorption spectrum of said fluorophore.

The purpose of the experiment was to produce a saturation curve by comparing the incoming laser intensity with the fluorescence intensity emitted from the sample. According to the simulation code in section 3.1, the laser intensity will be equivalent to the fluorescence intensity when the response curve is linear. Such a response curve corresponds to a case where saturation has not been reached, that is, where the fluorescence signal always increases with increasing laser intensity. Therefore, a picture was taken of the sample when irradiated with a laser intensity so low that saturation could be excluded. This picture could then be assumed to correspond to the incoming laser intensity.

Saturation of the sample was achieved by increasing the laser intensity in discrete, equally large steps using the Q-switch delay. One picture was taken after each increase with the software program Solis connected to the camera. Saturation curves were then produced by using the picture taken with the lowest laser intensity and a picture with one of the highest intensities and plotting them as described below.

3.4 Data processing code

The analysis code can be found in Appendix C. The purpose of this code was to extract the pictures of the irradiated fluorophores from the software Solis, plot the Fourier transforms of the laser and fluorescence signals, plot the saturation curve, and obtain the values of I_ν^{sat} and k, from Equation (10), for each fluorophore. Figure 7 show visual examples (created using the simulation code in Appendix B) of the of the laser signal, the fluorescence signal and the saturation curve created when the two signals are plotted against each other. To be able to extract the images and plot them in Python, the imshow command from the matplotlib.pyplot package was used. The values along the x-axis of each image were summed together and normalised. This normalised list was then plotted against an arbitrary x-axis.

The Fourier transforms of the laser and fluorescence intensities were plotted using the fft package from the SciPy library [14]. The saturation curves were created by plotting the list of summed values of the fluorescence intensities against the corresponding list of the laser intensities as a scatter plot. To obtain values for I_ν^{sat} and k, a numerical fit of the scatter plot was made. This fit was created using the curve_fit command in the scipy.optimize package together with Equation (10) [14].

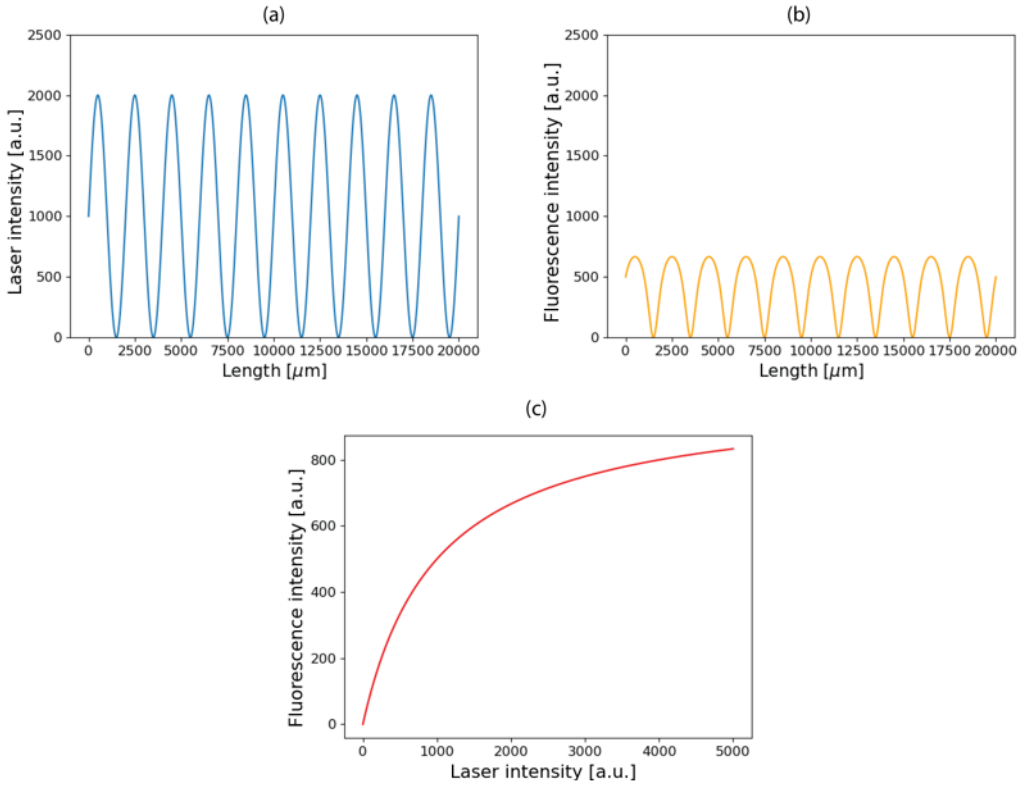

Figure 7: Three figures showing the two components necessary to create a saturation curve and the resulting curve. (a) shows the laser signal, (b) shows the fluorescence signal, and (c) shows the resulting saturation curve.

3.5 Initial experimental setup

The setup in this section did not manage to achieve saturation and was therefore replaced by the setup described in Section 3.2. Figures 16 and 17 in Appendix A show the setup described here.

In this setup, a 450 nm 2 W CW laser was used. A filter wheel and an additional filter, mounted on a component that can be flipped up and down, were attached to this laser to ensure laser safety. To create structured light, a DOE (not shown in Figures 16 and 17), was used. However, since the laser beam used to excite the fluorophore was narrow, only a small area of the sample could be illuminated by it. A telescope, consisting of a -25 mm negative lens and a 100 mm positive lens, was therefore used to magnify the beam. To create an image of the structured laser beam at the place of the sample, a 4-f imaging system was created using two positive lenses with focal lengths of 250 mm. An iris was placed in the Fourier plane of the 4-f imaging system to block the higher frequencies created by the DOE. Through this process, the laser beam was ensured to be sinusoidally modulated.

Backscattering was used to detect the fluorescence signal. The backscattered fluorescence signal was created using a polarizing beam splitter with a 45° angled mirror over it. The sample, located in a sample tray, was situated below the beam splitter. The part of the laser beam that went through the beam splitter down to the sample tray then excited the sample, resulting in backscattering fluorescence onto a camera placed in the setup.

4 Results and discussion

4.1 Saturation of different fluorophores

The results presented in this section were obtained using the setup described in Section 3.2. By using said setup it was possible to achieve saturation of several types of fluorophores. Discussions of the results are included in this section.

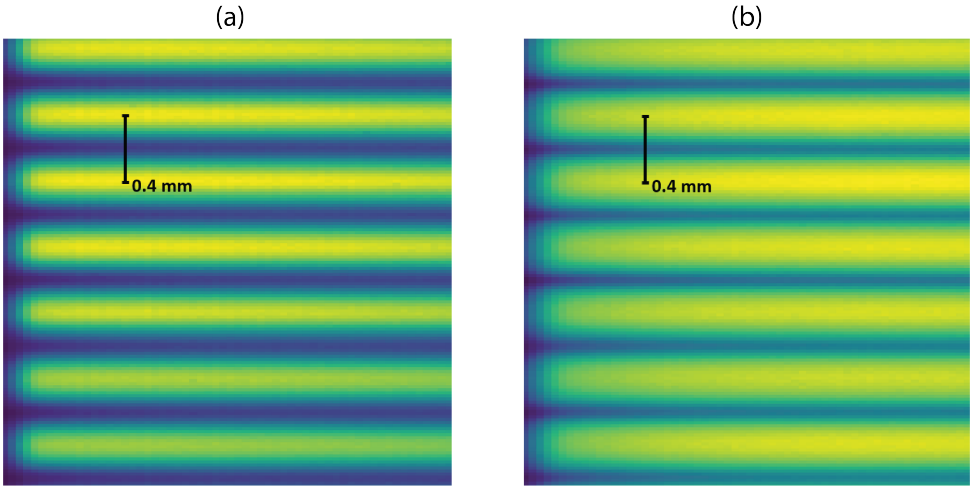

Figure 8: Pictures showing the difference in the sinusodial pattern between a non-saturated and a saturated sample of Rhodamine 560 in ethanol. (a) shows the non-saturated sample, while (b) shows the saturated sample.

The effect of saturation on the modulated sheet can be seen in Figures 8(a) and 8(b). There is a clear difference between these two pictures, which can be easily observed with the human eye. Figures 8(a) and 8(b) can be compared to Figure 4(e). The two patterns in the non-saturated and saturated sample mimic the different shapes of the curves shown in Figure 4(e). This indicates that the observed behaviour is close to the predicted behaviour, which strongly suggests that the observed distortion of the sine pattern is due to saturation.

Another indication that saturation was achieved is displayed in Figure 9. It can be seen that the saturated sample shows a larger number of peaks in the Fourier transform than the non-saturated one. A similar difference can be seen when comparing the Fourier transforms in Figures 5(a) and 5(c). This shows once again, that the observed behaviour is as predicted. The exact number of additional peaks can however not be compared, since the values of I_ν^{sat} and k are not the same in data produced by the simulation code and the actual data. Due to a fluorescence signal measured at low laser intensity being used as the laser signal, the Fourier transform of the non-saturated sample might not correspond to the one of a perfect sine wave, something that can be observed in Figure 9. However, Figure 9 shows that the higher order peaks are more distinct in the saturated case, thus justifying the reasoning of this paragraph.

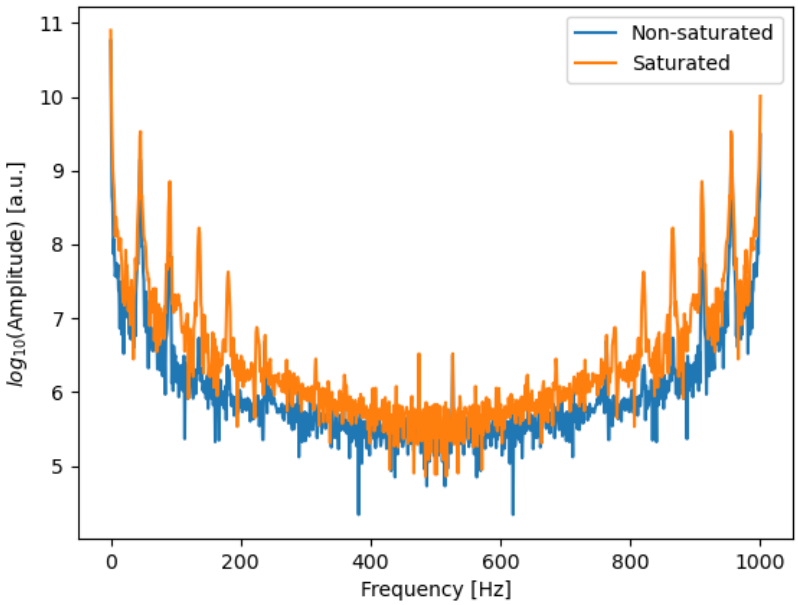

Figure 9: The Fourier transform of a non-saturated and saturated sample of Fluorescein.

4.1.1 Saturation curves of different fluorophores

To analyse the possible differences between the saturation curves for different fluorophores, the saturation curves for Rhodamine B, Fluorescein, Rhodamine 560, and Coumarin 153 were plotted using images obtained with the setup described in Section 3.2 and the analysis code described in Section 3.4. Figure 10(b) shows these saturation curves. The images used to create the curves are shown in Figure 10(a). It can be seen from Figure 10(b) that the saturation curves are visibly different for different compounds. The values of I_{532}^{sat} and k are shown in Table 1 for added clarity and to show the exact difference between the curves. This result clearly shows that the used method, which only utilises the properties of the elements and no spectroscopic technique, is useful to differentiate between different fluorophores. It is thus possible to tell several fluorophores apart using a single-shot method which includes a reference image.

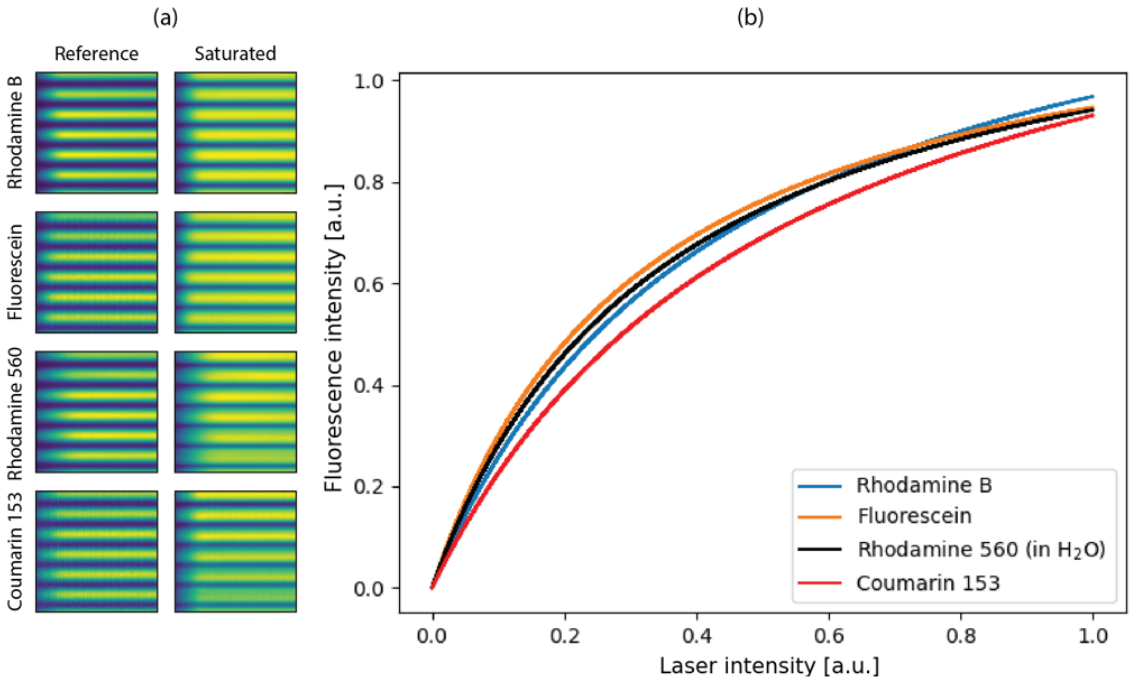

Figure 10: The saturation curves for four different fluorophores. (a) shows the pictures of the samples used to create the curves. (b) shows the saturation curves.

Fluorophore	**Conc. [mol/l]**	$\mathbf{I_{532}^{sat}}$ **[a.u.]**	**k**	$\lambda_{\mathbf{max}}$**[nm]**	$\boldsymbol{\tau}$ **[ns]**
Rhodamine B (in H_2O)	10^{-5}	0.443	1.397	554	1.75
Fluorescein (in H_2O)	10^{-4}	0.317	1.247	490	4.0
Rhodamine 560 (in H_2O)	10^{-4}	0.353	1.274	497	4.28
Coumarin 153 (in ethanol)	10^{-4}	0.533	1.426	421	4.85

Table 1: The values for I_{532}^{sat} and k for the saturation curves in Figure 10. The different values of I_{532}^{sat} are all comparable since all saturation curves have been normalised in the same way. Concentration, maximum absorption wavelength, λ_{max}, and lifetime, τ, of each fluorophore are also included [18, 19, 20, 21].

The two most similar saturation curves are the ones for Fluorescein and Rhodamine 560. These fluorophores also have the most similar values for I_{532}^{sat} and k according to Table 1. The saturation curve for Rhodamine B is decidedly different compared to the previous two curves, something that also is reflected in the values of I_{532}^{sat} and k. However, the saturation curve that differs visibly the most from the others is the curve for Coumarin 153. The values of I_{532}^{sat} and k for Coumarin 153 are higher than the corresponding values for all other fluorophores. The largest difference of I_{532}^{sat} and k can be observed when comparing the values for Fluorescein and Rhodamine 560 with the ones for Coumarin 153.

There are several differences in the properties of the fluorophores used to create Figure 10. Some of these properties, such as concentration, absorption wavelength, and lifetime are listed in Table 1. According to Table 1, the concentrations of Fluorescein, Rhodamine 560, and Coumarin 153 are all the same, while the concentration of Rhodamine B is ten times lower. This property seems to not be the main factor causing variation since the curve that varies the most is the one of Coumarin 153, which has the same concentration

as two of the other fluorophores. Due to the lack of quantitative data, however, it is not possible to draw this conclusion with certainty.

The maximum absorption wavelengths for the four fluorophores, which can be found in Table 1, vary when compared to each other. This observation implies that the absorption spectra, and thus the absorption cross sections, are different for the four fluorophores. The wavelengths for Fluorescein and Rhodamine 560 are close to each other, while the one from Rhodamine B differs a bit. The wavelength for Coumarin 153 differs the most.

The absorption cross section of an element indicates the probability of absorption of said element at different wavelengths. Here, the probability of absorption corresponds to the fluorescence intensity. The wavelength of the light source in this case is 532 nm emitted from the Nd:YAG pulsed laser. Thus, the closer the maximum absorption wavelength is to 532 nm, the higher the fluorescence intensity. According to this reasoning, Coumarin 153 should have the lowest fluorescence intensity, since its maximum absorption wavelength deviates the most from the laser wavelength of 532 nm. This is indeed the case, the saturation curve of Coumarin 153 has a less steep slope compared to the saturation curves of the other fluorophores, which here corresponds to lower values of fluorescence intensity. The observed connection between absorption cross section and saturation curves also suggests that fluorophores with similar maximum absorption wavelengths should have similar saturation curves due to alike fluorescence intensities. This behaviour can also be observed in Figure 10, where the saturation curves of Fluorescein and Rhodamine 560 are more similar compared to each other than to the other saturation curves.

Table 1 also includes the lifetimes of the four fluorophores. The lifetime of a fluorophore is the time that it spends in an excited state, before deexciting and emitting light in the form of a photon. Similarly to the reasoning regarding absorption cross sections, a connection can be drawn between the shape of the saturation curve and the lifetime since Equation (11) states that the emission rate from a fluorescent sample is dependent on the lifetime of the fluorophore. The lifetimes of Fluorescein and Rhodamine 560 are rather similar, although with a non-negligible difference. This difference is reflected in Figure 10, where the saturation curves belonging to these fluorophores are similar, but not identical. The lifetime of Rhodamine B differs the most compared to the other lifetimes. This is a likely factor as to why the saturation curve of Rhodamine B distinguishes itself from the other saturation curves. It can be observed that Rhodamine B has a maximum absorption wavelength which also differs noticeably from the corresponding wavelengths of Rhodamine 560 in water and Fluorescein. However, since the absorption spectra of these three fluorophores all contain the laser wavelength of 532 nm, it is unlikely that the difference in maximum absorption wavelength has a noticeable effect on the curves. Thus, the lifetime of the fluorophore seems to be a property that affects the saturation curve of said fluorophore considerably.

According to Equation (8), I_ν^{sat} depends on different Einstein coefficients, which in turn affect the populations of the ground state and the excited state. When saturation has been achieved, the fluorescence signal will not change due to a change in irradiance. By all of this reasoning, it is implied that saturation is reached when the excited state contains the maximum possible amount of fluorophore molecules. The probability of the excited state being filled increases the longer the lifetime is since it corresponds to the time the

molecule spends in the excited state. Therefore it follows that the highest probability of saturation should occur for the fluorophore with the longest lifetime. A high probability of saturation corresponds graphically to the saturation curve converging quickly. However, the saturation curves in Figure 10 does not fully converge. Because of that, their slopes at high intensities has to be studied to draw a conclusion.

Table 1 states that the longest lifetime is the one of Coumarin 153. In contradiction to this, the saturation curve of Coumarin 153 does not converge quickly compared to the other saturation curves in Figure 10, implying that Coumarin 153 is more difficult to saturate. The maximum absorption wavelength of Coumarin 153 is although significantly different compared to the laser wavelength, thus implying a low probability of absorption. It is thus possible that this latter property affects the fluorescence signal more than the lifetime in this case, and that the resulting signal, therefore, remains low.

Rhodamine 560 in water and Fluorescein both have longer lifetimes than Rhodamine B, and absorption spectra containing the laser wavelength. These two saturation curves can be seen to approach a constant value the quickest, thus justifying the reasoning above. It is difficult to determine which of these two saturation curves that approaches a constant value the quickest using just Figure 10. Therefore it is implied that the methods used need to be improved in order to experimentally confirm the reasoning made above.

Another property that varies between the fluorophores is the solvent. According to research, the solvent of a fluorophore has a noticeable effect on its absorption wavelength and lifetime [18]. Coumarin 153 has ethanol as a solvent, while the other three have water. This can therefore be a factor that results in the saturation curve of Coumarin 153 differentiating itself from the other saturation curves.

In conclusion, several physical properties seem to affect the saturation curve of a fluorophore, suggesting that saturation curves can be used for several purposes. More experiments need to be conducted in order to investigate exactly how the properties affect the shape of the curves.

4.1.2 Saturation and intensity distribution

Figure 11 shows four figures which were compared and analysed to investigate if the different intensity distributions could be connected to the absorption cross section. The samples used are Rhodamine 560 in ethanol and Fluorescein in water. Two of the figures, namely Figures 11(b) and 11(d) show the samples when saturated, while the other two figures show the non-saturated samples. The results from this analysis could then strengthen the connections between saturation curves and absorption cross section made in Section 4.1.1.

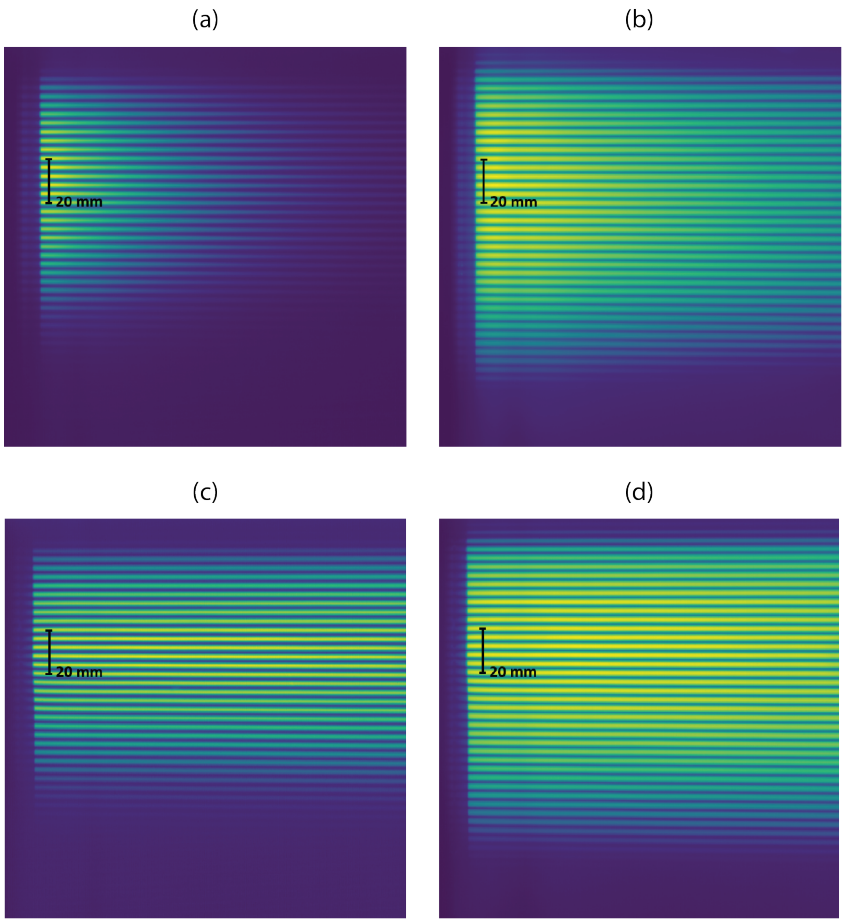

Figure 11: Pictures of non-saturated and saturated samples of Rhodamine 560 in ethanol and Fluorescein in water illustrating the different absorption rates of the two compounds. (a) and (b) show the non-saturated sample and saturated sample of Rhodamine 560 in ethanol respectively. (c) and (d) show the non-saturated sample and saturated sample of Fluorescein in water respectively.

There is a clearly visible difference between the shape of illumination when comparing Figures 11(a) and 11(b) with Figures 11(c) and 11(d). This can be interpreted as a difference in absorption rate between the two fluorophores. The absorption rate can, in turn, be related to the absorption cross section of the fluorophore in question, since this latter physical property gives the probability of absorption for a certain wavelength of the light source. The absorption of an element is described by the Beer-Lambert law, which can be expressed in the following way

$$\frac{I}{I_0} = \exp(-n_i \sigma_i L) \tag{15}$$

where I is the intensity of the emitted light, I_0 is the initial intensity, n_i is the concentration of the absorbing element, σ_i is the absorption cross section and L is the distance that the incoming beam travels through the sample [2]. I is here the fluorescence signal, while I_0 corresponds to the laser signal. L can be approximated to be the same for both fluorophores since the setup is identical in both cases. Due to the concentrations of the fluorophores also being the same according to Table 2, Figures 11(a), 11(b), 11(c) and 11(d) together with Equation (15) indicate that the absorption cross section σ_i is different

for Rhodamine 560 in ethanol and Fluorescein in water at 532 nm. Table 2 states that the maximum absorption wavelengths for these two fluorophores are different, justifying the reasoning above. The drawn conclusion is also strengthened by Figures 12(a) and 12(b), which display the change in intensity over the x-axis for the images in Figure 11.

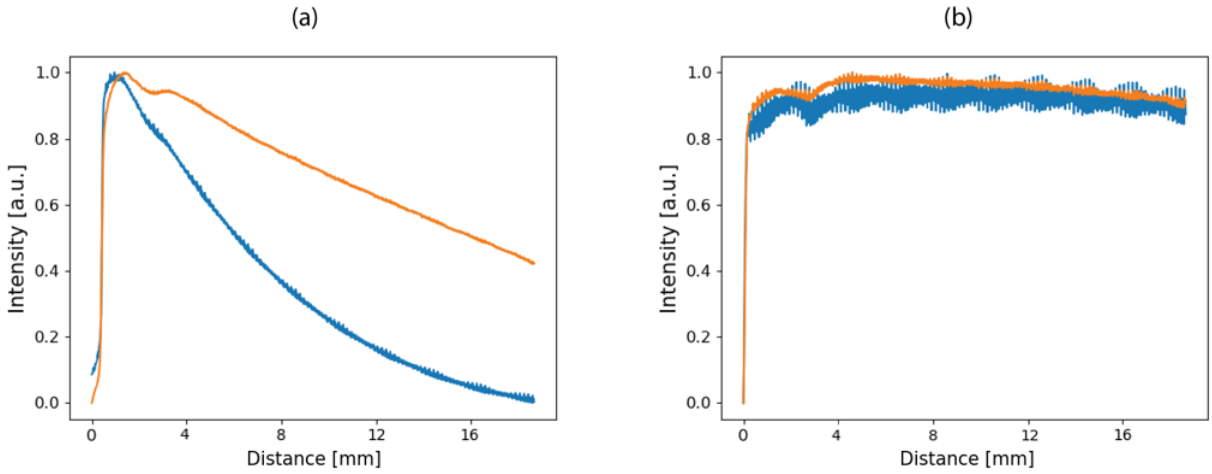

Figure 12: Plots illustrating the change in intensity over distance for non-saturated and saturated samples of Rhodamine 560 in ethanol and Fluorescein in water. The blue curves correspond to the non-saturated samples while the orange curves correspond to the saturated samples. (a) shows the intensity distribution for Rhodamine 560 in ethanol and (b) shows the intensity distribution for Fluorescein in water.

The blue curve in Figure 12(a), which shows the intensity distribution of the non-saturated sample of Rhodamine 560, has the shape of a negative exponential, which is exactly what Equation (15) is. Thus, Figure 12(a) shows that Figure 11(a) displays the same behaviour as the Beer-Lambert law. Comparing these results to the intensity distribution of the non-saturated sample of Fluorescein, shown as the blue curve in Figure 12(b), a clear difference in behaviour can be observed. This curve has a much smaller slope, although it has a slight negative slope. Thus, the sample of Fluorescein can also be assumed to follow the Beer-Lambert law, but with a decrease less rapid due to a smaller cross section. The radical difference in intensity distribution between the two discussed curves can be found in Figures 11(a) and 11(c) as well. The decrease in intensity in the first of these two figures is very clear, while the intensity distribution in the latter one is visibly constant. This observation further strengthens the argument that Rhodamine 560 in ethanol and Fluorescein in water have different absorption cross sections.

According to Table 2, the maximum absorption wavelength of Fluorescein in water differs more from the laser wavelength than the maximum absorption wavelength of Rhodamine 560 in ethanol. Therefore, this data implies that the absorption cross section at 532 nm is smaller for Fluorescein in water than Rhodamine 560 in ethanol; motivating the argument made in the paragraph above. It can however be observed that the maximum absorption wavelength of Rhodamine 560 in ethanol is very close to the corresponding wavelength of Fluorescein in water. Figures 11 and 12 thus suggest that a small difference in absorption cross section has a large impact on the intensity distribution of the sample.

It can be noted that the behaviour of the intensity decay of the saturated sample of

Rhodamine 560 in ethanol, represented by the orange curve in Figure 12(a), follows a nearly linear negative slope for the most of the sample. Since the blue curve, which represents the non-saturated case, has a steeper slope than the orange, it is implied that the decrease in intensity is slower in the saturated case. This argument is motivated by Figures 11(a) and 11(b). When comparing these figures it can be seen that the intensity is higher further along the x-axis in the saturated case than in the non-saturated case. The curves shown in Figure 12(b), display the intensity distribution of the saturated and non-saturated sample of Fluorescein in water. These curves are not as different from each other as the curves in Figure 12(a). However, the orange curve in Figure 12(b), corresponding to the saturated case, can be seen to have a slightly smaller slope at higher intensities compared to the blue curve. This observation is in agreement with the intensity distribution that can be seen in Figures 11(c) and 11(d).

As explained above, the decrease in intensity over space is more rapid in the non-saturated samples, than in the saturated ones. This behaviour is in accordance with the definition of saturated PLIF written in the theory, which states that the fluorescence intensity is constant in the saturated case. The fluorescence signal is then independent of the laser intensity. That is, if saturation has been achieved in parts of the sample, the fluorescence intensity should be equally large in these parts. Thus, the smaller slopes of the orange curves shown in Figures 12(a) and 12(b) further motivates that saturation was achieved, at least partially, in the conducted experiments. Due to the actual samples absorbing the incoming light from the laser, at some distance into the sample, the intensity of the incoming light will be too low to achieve saturation. This reasoning explains why there is a decrease in fluorescence intensity also in the saturated cases. The slower decrease in intensity in the saturated cases can also partly be explained by the presence of incoming light with a substantially higher intensity. There will then be a larger amount of photons, which will increase the illuminated area of the sample.

4.2 Saturation curves and lifetime

To further investigate how saturation curves depend on the lifetime of the sample, two fluorophores with the same lifetime were saturated. The chosen fluorophores were Rhodamine 560 with ethanol as solvent and Fluorescein with water as solvent. Saturation curves for the fluorophores were created by measuring the non-saturated and saturated states in both cases. The curves, which can be seen in Figure 13, are almost identical. The values of I_{532}^{sat} and k, displayed in Table 2, are very also close to each other in magnitude, thus strengthening the conclusion of the observation.

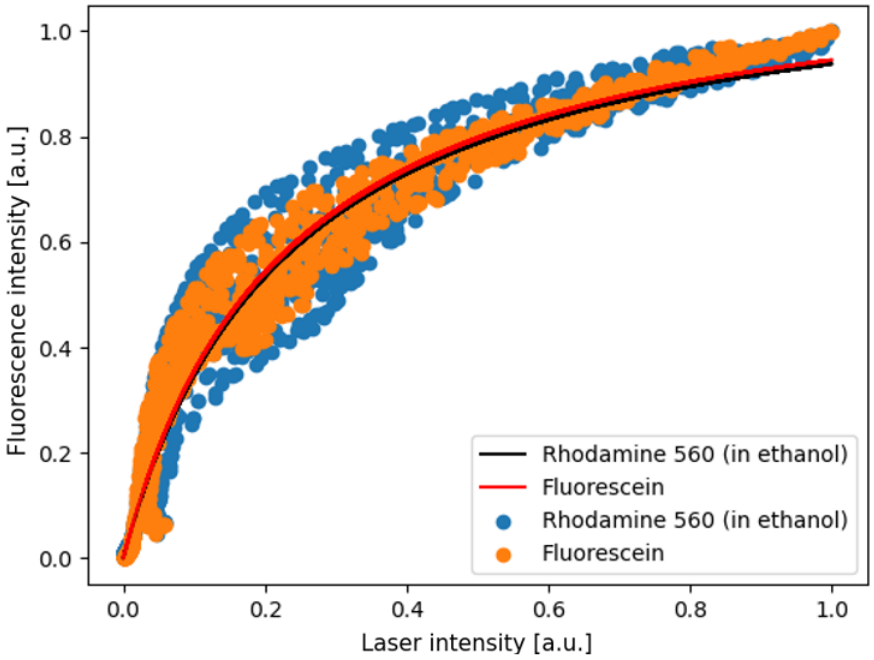

Figure 13: The saturation curves for Rhodamine 560 in ethanol and Fluorescein in water. The scatter plots consist of all of the data points in the pictures used for plotting.

Fluorophore	**Conc. [mol/l]**	$\mathbf{I_{532}^{sat}}$ **[a.u.]**	**k**	$\boldsymbol{\lambda_{max}}$**[nm]**	$\boldsymbol{\tau}$ **[ns]**
Rhodamine 560 (in ethanol)	10^{-4}	0.233	1.156	499	4.00
Fluorescein (in H_2O)	10^{-4}	0.226	1.159	490	4.0

Table 2: The values for I_{532}^{sat} and k for the saturation curves in Figure 13. The lifetimes, τ, and the concentrations for the two fluorophores are also shown along with their maximum absorption wavelengths, λ_{max} [18, 19, 21].

As mentioned in Section 4.1, Equation (11) shows that the fluorescence signal from a sample is dependent on the lifetime of the fluorophore in that sample. In that section, it was also observed that the lifetimes and saturation curves of Rhodamine 560, with water as a solvent, and Fluorescein, with the same solvent, were rather similar, but still had a noticeable difference. The two previous sections concluded that the absorption cross section of a fluorophore heavily affects the saturation curve of said fluorophore. However, the maximum absorption wavelengths of Rhodamine 560 in ethanol and Fluorescein in water differ more than the corresponding wavelengths of Rhodamine 560 in water and Fluorescein in water. This information contradicts the fact that the saturation curves of Rhodamine 560 in ethanol and Fluorescein in water are more similar to each other. Therefore it must be that the lifetimes of the fluorophores clearly affect the shape of their saturation curves.

According to Table 2, the concentrations of Rhodamine 560 in ethanol and Fluorescein in water are identical. However, this was also the case for Rhodamine 560 in water and Fluorescein in water in Table 1, despite the values of I_{532}^{sat} and k varying more in that case. Thus, the main reason for the similarities between the values of I_{532}^{sat} and k in Table 2 has to be their identical lifetimes. This conclusion has several interesting implications. If the

method used in this project could be utilised to find the lifetimes of fluorophores, it will be a highly efficient method for biomedical applications where the fluorescence lifetime can provide valuable information about the sample.

4.3 Multiple fluorophores in a single shot

To analyse if the method used in this project could be made more efficient, an experiment was conducted where two different fluorophores were irradiated simultaneously. During the experiment, two smaller cuvettes containing Rhodamine B and Fluorescein were placed next to each other in such a way that both cuvettes were in the camera's field of view. This resulted in images containing two samples. Figure 14 shows the non-saturated and saturated cases.

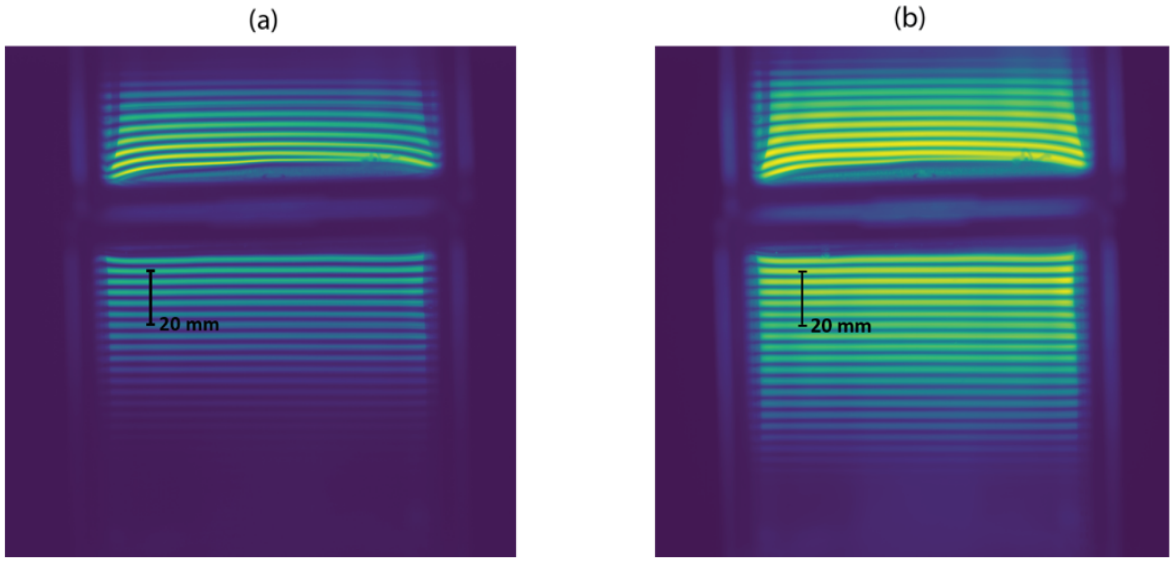

Figure 14: Pictures including two cuvettes containing different compounds, in this case Fluorescein (above) and Rhodamine B (below). (a) displays the picture of the non-saturated samples and (b) displays the picture of the saturated samples.

It was possible to construct separate saturation curves for the two fluorophores using only the images shown in Figure 14, by using different parts of the image for each calculation. The images were then cropped during the data analysis before the saturation curves were plotted. The resulting saturation curves are shown in Figure 15. This is, to the knowledge of the author, the first time that saturation curves for two different fluorophores have been produced using just two snapshots in total; where one of them is for reference. Compared with previous methods of creating saturation curves, the method used in this experiment is drastically more efficient. These successful results show once again that the method presented in this project, where saturated PLIF is conducted with structured light, could have many areas of applications. If developed and improved, experiments such as the one discussed in this section could be performed with three or more different samples. A highly effective and also relatively simple method of identifying fluorophores would then have been created. There are however some factors that need to be altered in order to obtain an optimized method.

When imaging several cuvettes simultaneously, a wide laser sheet is sought after. The wider the sheet, the more cuvettes will be contained in the image. A telescope, similar to the one described in Section 3.5, was therefore installed between the laser and the DOE to magnify the sheet. During measurements, however, it was noted that saturation could not be achieved when the telescope was used, despite increasing the intensity of the laser to its maximum level. A likely reason for this issue is that the magnification results in too large intensity losses. The range of laser intensities in the used laser is then too small to yield intensities high enough to achieve saturation.

According to Equations (11) and (13), the shorter the pulse of the laser, the more effective the laser is to achieve saturation. Equation (10) states that the intensity of the laser has to be substantially larger than the saturation intensity for saturation to be achieved. These statements, together with the reasoning above, suggest that a large range of intensities is needed to achieve saturation if a certain magnification is utilised. It might thus be possible to achieve saturation with a magnified laser sheet if a pico- or femtosecond laser is used instead. The range of intensities would then be larger than in the case of the nanosecond laser used in the measurements. Further investigation is needed to determine if this is possible and how large the magnification then can be.

Several difficulties due to the physical properties of the samples were noted during the experiment. One of these was a capillary effect in the corners of the cuvettes. This effect was not observed when conducting experiments with the same fluorophores in the larger cuvette, shown in Figure 6. Due to the capillary effect, the lines were disrupted, making it more difficult to extract reliable data for producing the saturation curves. The capillary effect can be seen in Figures 14(a) and 14(b); mostly in the sample of Fluorescein. Since there is a clear difference in how pronounced this issue is between the sample of Rhodamine B and the sample of Fluorescein, the behavior is most probably due to molecular properties. Another observed difficulty was the necessity of using samples with the same fluorescence intensity. When irradiating two samples, one with higher fluorescence intensity than the other, the one with lower intensity would emit too weakly to be visible. This was discovered to be a sensitive property; a small difference in fluorescence intensity would result in the consequences mentioned.

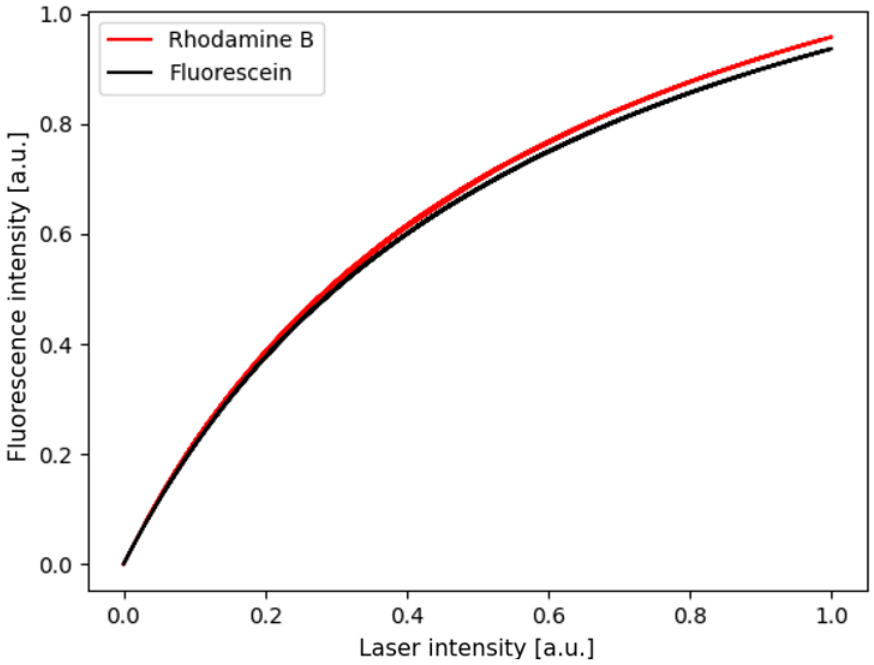

Figure 15: Saturation curves for Rhodamine B and Fluorescein produced using the pictures including both compounds.

Fluorophore	**Conc. [mol/l]**	$\mathbf{I_{532}^{sat}}$ **[a.u.]**	**k**	$\lambda_{\mathbf{max}}$**[nm]**	$\boldsymbol{\tau}$ **[ns]**
Rhodamine B (in H_2O)	10^{-6}	0.586	1.519	554	1.75
Fluorescein (in H_2O)	10^{-4}	0.592	1.491	490	4.0

Table 3: The values for I_{532}^{sat} and k for the saturation curves in Figure 15. The concentration, maximum absorption wavelength, λ_{max}, and lifetime, τ, of Rhodamine B and Fluorescein are also included.

Table 3 shows the values for I_{532}^{sat} and k belonging to the saturation curves in Figure 15, along with the concentrations, absorption wavelengths and lifetimes of the two fluorophores. Despite the concentration of Fluorescein being the same as in Table 1, the values of I_{532}^{sat} and k are quite different. This deviation of the values of I_{532}^{sat} and k can also be observed for Rhodamine B. In that case, however, the concentration is ten times lower compared to the sample of Rhodamine B listed in Table 1. Due to these dissimilarities, it can be concluded that the method in its present state gives unreliable data. This can be connected to the difficulties with the method mentioned above.

It is possible to improve the method for it to yield more certain data. By replacing the small cuvettes with another type of small cuvette that have a larger distance between its corners, the capillary effect could be avoided. If magnification of the laser sheet can be achieved during saturation using a pico- or femtosecond laser, it might be possible to use larger cuvettes and still contain several samples in one image; once again avoiding the capillary effect.

4.4 Difficulties with the former setup

The setup used prior to the one described in Section 3.2 was unable to achieve saturation. This setup is described in Section 3.5 and figures of it are shown in Appendix A. Several reasons for the difficulties experienced during the usage of this setup will now be discussed.

The former setup used a continuous laser instead of a pulsed one. According to Equation (11), it is more difficult to achieve saturation with a long-pulsed laser. A continuous laser can be seen as a laser with infinite pulse lengths. Thus, the utilising of a continuous laser could be the reason that saturation was not reached using this setup. During the experimental process, a telescope was used to magnify the beam, again without any success in reaching saturation. The reason for this is most probably the same as the one described in Section 4.3, namely that the available laser intensities are too low to achieve saturation.

A laser beam was used in the former setup instead of a laser sheet. A laser sheet can be focused at the location of the fluorophore, without resulting in an irradiated area that is too small, because it expands in two dimensions. If a laser beam is focused, the irradiated area will become so small that an image obtained from such an experiment would be useless. It is thus possible to maximize the intensity per area using a laser sheet, by irradiating the fluorophore with a higher intensity and promoting saturation. The usage of a beam instead of a sheet could therefore be one of the problems regarding achieving saturation.

The sample holder used in the former setup contained small indents for storing the fluorophores, which were around 1 cm^2. This arrangement, together with the usage of a laser beam instead of a sheet, resulted in very few lines from the laser per image. The amount of quantitative data was therefore low, yielding unreliable results. The image and plot quality improved drastically when changing to the larger cuvettes.

5 Conclusion

Saturation curves of four different fluorophores, namely Rhodamine B, Rhodamine 560, Fluorescein, and Coumarin 153 were successfully obtained with only two snapshots of each fluorophore, using the method explained in Sections 3.2, 3.3, and 3.4. Values for I_ν^{sat} and k, from Equation 10, were obtained for these curves and showed clear differences between the saturation curves of the fluorophores. It has thus been shown that saturation curves are unique for every fluorophore. This clearly suggests that saturation curves could be used as a way to differentiate between fluorophores. In the cases where two fluorophores have nearly identical absorption and emission spectra, saturation curves could be used to tell the two fluorophores apart. This method, especially if successfully converted into a single-shot method, would be drastically more effective and simple than the other methods available for differentiating fluorophores with similar absorption and emission spectra. Improvements of the current method would however be necessary in order to obtain fully reliable data.

Additional to this information, a visible difference between the curves could be observed in Figure 10. From these saturation curves and values, it was concluded that said parameters are heavily influenced by the absorption cross section and lifetime of the studied

fluorophores. The connection to the absorption cross section was further analysed by investigating the spatial intensity profile of the irradiated fluorophores. The dependence on lifetime was studied by plotting the saturation curves of two fluorophores with identical lifetimes. The saturation curves of these fluorophores were found to be nearly identical. Furthermore, experiments with two samples in a single shot were made. Saturation curves of both samples were successfully created using one image of the saturated samples and one reference image. In general, this method shows great potential and is worth investigating further.

6 Outlook

The experiments conducted in this project have many possibilities for usage in research. Since this method never has been conducted before, the success in obtaining saturation curves has opened up a whole new area of research regarding saturated PLIF and saturated LIF. Several improvements can be made for the method to be of use in further research.

At its present stage, the method requires two images to produce a saturation curve; one reference image, and one image of the sample in its saturated state. Because of that, it is not a true single-shot method. However, several possible ways can be utilised to convert it to a single-shot method. A theoretical sine wave, created in Python for example, could replace the reference image. Another possibility is to extract the initial sine wave from an image of the saturated sample through data analysis, thereby using only one image. More experimental ways of converting the current method into a single-shot method would be to install a beam-analysis tool, or a continuous laser which is imaged, before the sample. Using that, two figures would still be needed, but they would both be obtained using just one measurement of the sample. A continuous laser is then assumed to be unable to saturate the type of fluorophores used in the conducted experiments. If conversion to a single-shot method would succeed, the method would become more effective and attractive from a research perspective.

The saturation curves presented in the results show a distinct dependence on the lifetimes of the fluorophores used to produce said saturation curves. This conclusion is interesting for further research since the lifetimes of fluorophores are a wide and popular topic in present research. If saturation curves could be used to obtain the lifetimes of different fluorophores, this project would have proposed a very efficient method for measuring lifetimes.

Experiments with a pico- or femtosecond laser are planned to be conducted utilising the method and setup used in this project. Therefore, this project will be a source for future publications. Improvements of said method and setup will be performed before conducting experiments with the new laser. These planned experiments could investigate whether magnification of the beam is possible with the shorter pulse length, since short-pulsed lasers are supposed to be more beneficial in achieving saturation. It remains to see what these new experiments will discover. Hopefully, the method proposed in this project will become a new laser-diagnostic method with several areas of use.

References

[1] Chaze W, Caballina O, Castanet G, Lemoine F. The saturation of the fluorescence and its consequences for laser-induced fluorescence thermometry in liquid flows. Experiments in Fluids. 2016;57:1-18.

[2] Eckbreth AC. Laser diagnostics for combustion temperature and species. vol. 3. CRC press; 1996.

[3] Daily JW. Saturation effects in laser induced fluorescence spectroscopy. Applied Optics. 1977;16(3):568-71.

[4] Schäfer M, Ketterle W, Wolfrum J. Saturated 2D-LIF of OH and 2D determination of effective collisional lifetimes in atmospheric pressure flames. Applied Physics B. 1991;52:341-6.

[5] Kristensson E. Structured laser illumination planar imaging SLIPI applications for spray diagnostics. Lund University; 2012.

[6] Gustafsson MG. Nonlinear structured-illumination microscopy: wide-field fluorescence imaging with theoretically unlimited resolution. Proceedings of the National Academy of Sciences. 2005;102(37):13081-6.

[7] Mrkvičková M, Dvořák P, Svoboda M, Kratzer J, Voráč J, Dědina J. Dealing with saturation of the laser-induced fluorescence signal: An application to lead atoms. Combustion and Flame. 2022;241:112100.

[8] Kirby BJ, Hanson RK. CO 2 imaging with saturated planar laser-induced vibrational fluorescence. Applied Optics. 2001;40(33):6136-44.

[9] Kristensson E, Araneo L, Berrocal E, Manin J, Richter M, Aldén M, et al. Analysis of multiple scattering suppression using structured laser illumination planar imaging in scattering and fluorescing media. Optics express. 2011;19(14):13647-63.

[10] Pan C, Li L, Cao H, Zhao Y, Liu Y, Dai X. The design method of beam splitting based on DOE and its application in 3D imaging Lidar. In: AOPC 2022: Atmospheric and Environmental Optics. vol. 12561. SPIE; 2023. p. 49-60.

[11] Young HD, Freedman RA. University Physics with Modern Physics. vol. 15. Split nordics ed. Pearson; 2020.

[12] Saleh BE, Teich MC. Fundamentals of photonics. john Wiley & sons; 2019.

[13] Python. The Python programming language; 2023. [Online; accessed 10-May-2023]. Available from: `https://www.python.org/`.

[14] SciPy. The SciPy Python library; 2023. [Online; accessed 10-May-2023]. Available from: `https://scipy.org/`.

[15] Quantel Laser. Q-smart (850 mJ); 2023. [Online; accessed 10-May-2023]. Available from: `https://www.quantel-laser.com/en/products/item/q-smart-850-mj-.html`.

[16] Andor Technology. Andor Technology Luca S - Specification Sheet; 2008. [Online; accessed 10-May-2023]. Available from: https://www.affichez-vous.com/pdf/Andor_Luca-S_658M_Specifications.pdf.

[17] Edmund Optics Inc. GoldTL™ Telecentric Lens; 2023. [Online; accessed 10-May-2023]. Available from: https://www.edmundoptics.com/f/goldtl-telecentric-lenses/11863/.

[18] Zhang XF, Zhang Y, Liu L. Fluorescence lifetimes and quantum yields of ten rhodamine derivatives: Structural effect on emission mechanism in different solvents. Journal of luminescence. 2014;145:448-53.

[19] Doughty MJ. pH dependent spectral properties of sodium fluorescein ophthalmic solutions revisited. Ophthalmic and Physiological Optics. 2010;30(2):167-74.

[20] Baumann R, Ferrante C, Kneuper E, Deeg FW, Bräuchle C. Influence of confinement on the solvation and rotational dynamics of coumarin 153 in ethanol. The Journal of Physical Chemistry A. 2003;107(14):2422-30.

[21] Berezin MY, Achilefu S. Fluorescence lifetime measurements and biological imaging. Chemical reviews. 2010;110(5):2641-84.

A Previous setup

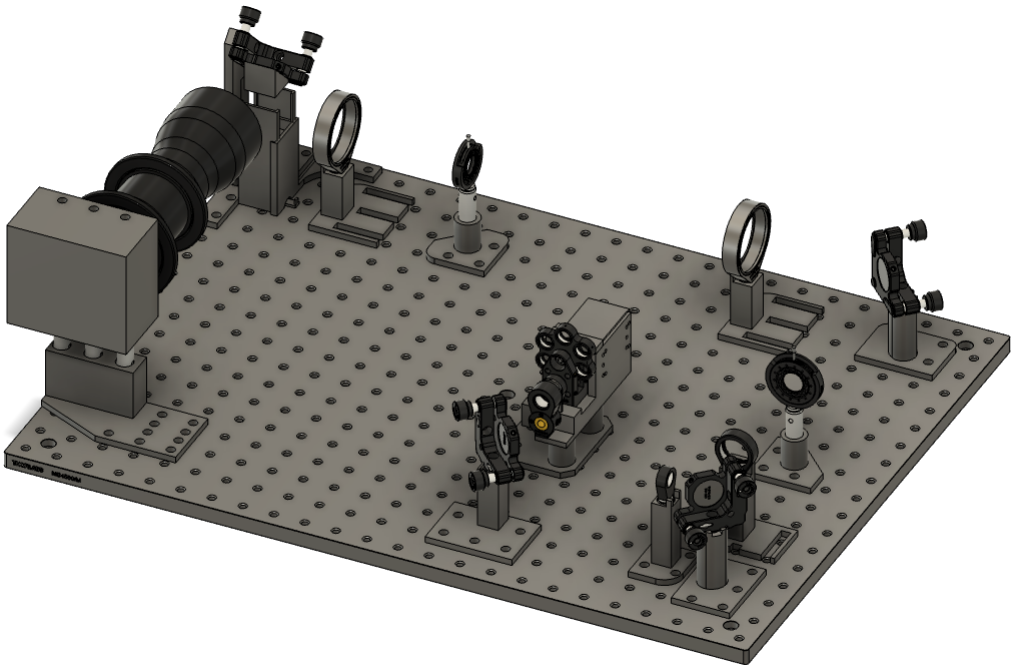

Figure 16: The experimental setup from the side.

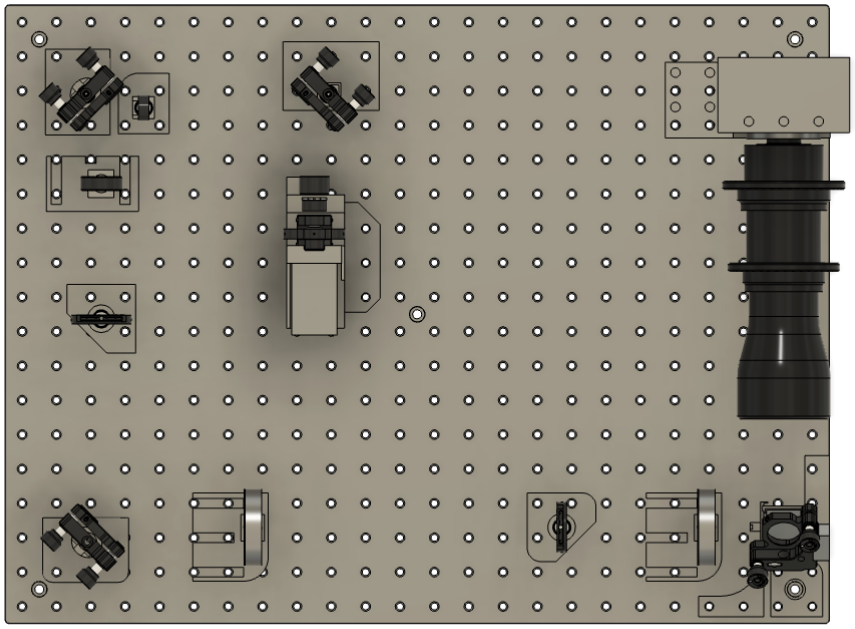

Figure 17: The experimental setup from above.

B Simulation code

```
import numpy as np
import matplotlib.pyplot as plt
from scipy import fftpack

#Nr of measurements
N = 20000
#Angular frequency
v = (2*np.pi*10)/N
k = 1000
IinMin = 0
#Maximum amplitude of incoming light
IinMax = 2000
#The intensity required for achieving saturation
I_sat = 0.5*IinMax
#The largest value on the x-axis of the saturation curve
Iintot = 5000

#Spatial values for the incoming sine wave
xL = np.linspace(0,N,N)
#Incoming sine wave
L = IinMax*0.5*(np.sin(v*xL) + 1)
#X-axis for the saturation curve
L_tot = np.linspace(0,Iintot,N)

#Linear response curve
Iut_lin = L
Iut_lin_tot = L_tot

#Square-root response curve
Iut_sqrt = k*np.sqrt(L/1000)
Iut_sqrt_tot = k*np.sqrt(L_tot/1000)

#Non-linear response curve (the one that we change the max x-value of)
Iut = k*(1/(1+(I_sat/L)))
#Y-axis for the model of the response curve
Iut_tot = k*(1/(1+(I_sat/L_tot)))

plt.figure(0)
#Plot incoming sine wave L
plt.plot(xL,L, label=('Incoming light'))
plt.xlabel('Length [$\mu$m]')
plt.ylabel('Intensity [a.u.]')
plt.title('Intensity of incoming and outgoing light')
#Plot outgoing distorted sine wave Iut from linear response curve
# plt.plot(xL,Iut_lin, label=('Outgoing light'))
#Plot outgoing distorted sine wave Iut from square-root response curve
# plt.plot(xL,Iut_sqrt, label=('Outgoing light'))
#Plot outgoing distorted sine wave Iut from non-linear response curve
plt.plot(xL,Iut, label=('Outgoing light'))
plt.legend()
plt.ylim(0,2500)

plt.figure(1)
#Plot the model of the response curve (linear response curve)
# plt.plot(L_tot,Iut_lin_tot)
```

```
#Plot the model of the response curve (square-root response curve)
# plt.plot(L_tot,Iut_sqrt_tot)
#Plot the model of the response curve (non-linear response curve)
plt.plot(L_tot,Iut_tot)
plt.xlabel('Intensity [a.u.]')
plt.ylabel('Intensity [a.u.]')
plt.title('Response curve')

#Plot the actual experimental response curve
#Linear response
# plt.plot(sorted(L),sorted(Iut_lin))
#Square-root response
# plt.plot(sorted(L),sorted(Iut_sqrt))
#Non-linear response
plt.plot(sorted(L),sorted(Iut))

#Fourier transform of the outgoing modified sine wave (linear)
yf_lin = fftpack.fft(Iut_lin)
xf_lin = fftpack.fftfreq(Iut_lin.size, d=1/N)
#Fourier transform of the outgoing modified sine wave (square-root)
yf_sqrt = fftpack.fft(Iut_sqrt)
xf_sqrt = fftpack.fftfreq(Iut_sqrt.size, d=1/N)
#Fourier transform of the outgoing modified sine wave (non-linear)
yf = fftpack.fft(Iut)
xf = fftpack.fftfreq(Iut.size, d=1/N)
plt.figure(2)
#Linear
# plt.plot(xf_lin, abs(yf_lin))
#Square-root
# plt.plot(xf_sqrt, abs(yf_sqrt))
#Non-linear
plt.plot(xf, abs(yf))
plt.xlim(-100,100)
plt.xlabel('Frequency [Hz]')
plt.ylabel('Amplitude [a.u.]')
plt.title('Fourier transform of the outgoing light')
```

C Data analysis code

```
import numpy as np
import matplotlib.pyplot as plt
from astropy.io import fits
from scipy import fftpack
import scipy
from scipy.optimize import curve_fit
import os

#Open files
os.chdir(r'C:\Users\klara\Desktop\Kandidatarbete\rh 560 in ethanol')
hdulist_sat_1 = fits.open("110.fits")
hdulist_nosat_1 = fits.open("160.fits")

os.chdir(r'C:\Users\klara\Desktop\Kandidatarbete\fl')
hdulist_sat_2 = fits.open("110 2.fits")
hdulist_nosat_2 = fits.open("160 2.fits")
```

```
17
18 #Extract data
19 sat_data_1 = hdulist_sat_1[0].data
20 nosat_data_1 = hdulist_nosat_1[0].data
21
22 sat_data_2 = hdulist_sat_2[0].data
23 nosat_data_2 = hdulist_nosat_2[0].data
24
25 #Reshape data from 3D to 2D
26 new_sat_data_1 = np.reshape(sat_data_1,(1002,1004))
27 new_nosat_data_1 = np.reshape(nosat_data_1,(1002,1004))
28
29 new_sat_data_1 = new_sat_data_1[450:550,150:200]
30 new_nosat_data_1 = new_nosat_data_1[450:550,150:200]
31
32 new_sat_data_2 = np.reshape(sat_data_2,(1002,1004))
33 new_nosat_data_2 = np.reshape(nosat_data_2,(1002,1004))
34
35 new_sat_data_2 = new_sat_data_2[400:500,150:200]
36 new_nosat_data_2 = new_nosat_data_2[400:500,150:200]
37
38 #Plot the images of the samples
39 plt.figure(0)
40 plt.plot(new_sat_data_1)
41 plt.imshow(new_sat_data_1, extent=[-1, 1, -1, 1])
42 plt.title('Saturated sample 1')
43 plt.figure(1)
44 plt.plot(new_nosat_data_1)
45 plt.imshow(new_nosat_data_1, extent=[-1, 1, -1, 1])
46 plt.title('Non-saturated sample 1')
47 plt.show()
48
49 plt.figure(2)
50 plt.plot(new_sat_data_2)
51 plt.imshow(new_sat_data_2, extent=[-1, 1, -1, 1])
52 plt.title('Saturated sample 2')
53 plt.figure(3)
54 plt.plot(new_nosat_data_2)
55 plt.imshow(new_nosat_data_2, extent=[-1, 1, -1, 1])
56 plt.title('Non-saturated sample 2')
57 plt.show()
58
59 #Sum the elements of the fist axis
60 flattenedSat_1 = np.sum(new_sat_data_1,axis=1)
61 flattenednoSat_1 = np.sum(new_nosat_data_1,axis=1)
62
63 flattenedSat_2 = np.sum(new_sat_data_2,axis=1)
64 flattenednoSat_2 = np.sum(new_nosat_data_2,axis=1)
65
66 #Normalise the sums
67 flattenedSat_1 = flattenedSat_1/max(flattenedSat_1)
68 flattenednoSat_1 = flattenednoSat_1/max(flattenednoSat_1)
69
70 flattenedSat_2 = flattenedSat_2/max(flattenedSat_2)
71 flattenednoSat_2 = flattenednoSat_2/max(flattenednoSat_2)
72
73 #Plot the summed and normalised intensities
```

```
norm_flattenedSat_1 = (flattenedSat_1 - min(flattenedSat_1))/max(flattenedSat_1 - min(flattenedSat_1))
norm_flattenednoSat_1 = (flattenednoSat_1- min(flattenednoSat_1))/max(flattenednoSat_1 - min(flattenednoSat_1))

norm_flattenedSat_2 = (flattenedSat_2 - min(flattenedSat_2))/max(flattenedSat_2 - min(flattenedSat_2))
norm_flattenednoSat_2 = (flattenednoSat_2 - min(flattenednoSat_2))/max(flattenednoSat_2 - min(flattenednoSat_2))

plt.figure(4)
plt.plot(flattenedSat_1,label='Saturated')
plt.plot(norm_flattenedSat_1,label='Non-saturated')
plt.legend()
plt.title('Intensity of sample 1')
plt.xlabel('Length [Pixels]')
plt.ylabel('Intensity [a.u.]')

plt.figure(5)
plt.plot(norm_flattenedSat_2,label='Saturated')
plt.plot(norm_flattenednoSat_2,label='Non-saturated')
plt.legend()
plt.title('Intensity of sample 2')
plt.xlabel('Length [Pixels]')
plt.ylabel('Intensity [a.u.]')

#Plot the logarithms of the Fourier transforms to get a useful scale
plt.figure(6)
plt.plot(np.log10(abs(fftpack.fft(flattenedSat_1))),label='Saturated')
plt.plot(np.log10(abs(fftpack.fft(flattenednoSat_1))),label='Non-saturated')
plt.legend()
plt.title('Fourier transform of intensity 1')
plt.xlabel('Frequency [Hz]')
plt.ylabel(r'$log_{10}$(Amplitude) [a.u.]')

plt.figure(7)
plt.plot(np.log10(abs(fftpack.fft(flattenedSat_2))),label='Saturated')
plt.plot(np.log10(abs(fftpack.fft(flattenednoSat_2))),label='Non-saturated')
plt.legend()
plt.title('Fourier transform of intensity 2')
plt.xlabel('Frequency [Hz]')
plt.ylabel(r'$log_{10}$(Amplitude) [a.u.]')

#Plot scatter plots of the saturation curves and numerical fits for these

def model_func(I, I_sat, k):
    return k*(1/(1+(I_sat/I)))

popt_1, pcov_1 = scipy.optimize.curve_fit(model_func, norm_flattenednoSat_1, norm_flattenedSat_1)
popt_2, pcov_2 = scipy.optimize.curve_fit(model_func, norm_flattenednoSat_2, norm_flattenedSat_2)
print('I_sat_1 = ', popt_1[0],', k_1 = ', popt_1[1])
print('I_sat_2 = ', popt_2[0],', k_2 = ', popt_2[1])

plt.figure(8)
plt.plot(norm_flattenednoSat_1, model_func(norm_flattenednoSat_1, popt_1[0], popt_1[1]), color='red')
```

```
125 plt.plot(norm_flattenednoSat_2, model_func(norm_flattenednoSat_2, popt_2[0], popt_2
        [1]), color='black')
126
127 plt.scatter(norm_flattenednoSat_2,norm_flattenedSat_2)
128 plt.title('Saturation curve')
129 plt.xlabel('Incoming intensity')
130 plt.ylabel('Outgoing intensity')
```